Online ISSN 3007-3197
Print ISSN 3007-3189
http://amresearchreview.com/index.php/Journal/about
Annual Methodological Archive Research Review
http://amresearchreview.com/index.php/Journal/about
Volume 3, Issue 5 (2025)

LWT Based Pre-coded Localized-OFDMA Technique for PAPR Reduction

[1]Nasir Mehmood Bahadar, [2]Arbab Waheed Ahmed, [3]Mazhar Islam, [4]Muhammad Asad Khan*, [5]Mohsin Khan, [6]Basir Usman

Article Details

Keywords: Fourier Transforms, Orthogonal Frequency Division Multiple Access (OFDMA), Long Term Evolution-Advanced (LTE-A), 5G communication, Peak to Average Power Ratio (PAPR), Bit Error Rate (BER).

Nasir Mehmood Bahadar
nasir.mehmood@hu.edu.pk
Arbab Waheed Ahmed
waheed.arbab@fecid.paf-iast.edu.pk
Mazhar Islam
mazharislam@hu.edu.pk
Muhammad Asad Khan *(Corresponding Author)
asadkhan@hu.edu.pk
Mohsin Khan
Mohsin_btn@yahoo.com
Basir Usman
usman.basir@gmail.com

ABSTRACT

Orthogonal Frequency Division Multiple Access (OFDMA) is choice of the day for many attractive features like high data rate communication and better spectral efficiency in multi path fading. However, OFDMA signal is greatly influenced by High Peak to Average Power Ratio (PAPR). Among numerous techniques, the Pre- coding based OFDMA techniques got more attention in terms of Bandwidth utilization, BER performance, PAPR reduction and Complexity. In this paper, a Lifting based Discrete Wavelet Transform (LWT) pre-coded localized-OFDMA (LOFDMA) technique is proposed for PAPR reduction in LTE-A/5G. The planned technique is equated with the conventional FFT based LOFDMA, conventional DWT based LOFDMA and the FFT pre-coded LOFDMA (SC-FDMA) techniques in terms of PAPR, BER, complexity, bandwidth usage and multi carrier communication using 8-QAM, 16-QAM and 64-QAM modulation schemes over Rayleigh fading channel. Through extensive simulations, it is shown that the proposed technique gives 58.82% improvement in PAPR reduction than conventional FFT-LOFDMA technique. Also, the suggested techniques has 73% better performance regarding BER as compared to the FFT pre-coded LOFDMA. The proposed technique is bandwidth efficient, moreover, its complexity compromise is very negligible as compared to conventional FFT-LOFDMA and conventional DWT-LOFDMA.

DOI: Availability

Introduction

Third Generation Partnership Project (3GPP) in its 8th release in 2004 introduced Long Term Evaluation (LTE) and later upgraded it to the Long Term Evolution-Advanced (LTE-A) in its 10th release in 2009 [1], [2]. LTE-A offers widespread coverage and global connectivity, representing a broadly implemented infrastructure [3], [4]. It is considered as the leading choice for device interconnection and is set as the foundation stone for the fu- ture development of 5G and the Internet of Things (IoT) [5]. Working within the frequency spectrum of 1.4 MHz to 20 MHz (including options such as 1.5 MHz, 3 MHz, 5 MHz, 10 MHz, 15 MHz, and 20 MHz), LTE grants a flexible approach to allocate frequency [6]. OFDMA as a multiple access scheme, is considered to be the preeminent choice of trans- mission for LTE/LTE-A standards because it is the best among multicarrier modulation schemes to achieve the targets of International Telecommunication Union (ITU) [7]. It ensures reliability in multipath fading environment [8]. Furthermore, OFDMA assists the simultaneous transmission of multiple users by assigning specific subgroups of spectrum to individual users [9]. This allocation is designed to each user's conditions, guaranteeing the effective consumption of radio resources, as illustrated in Figure 1 [10].

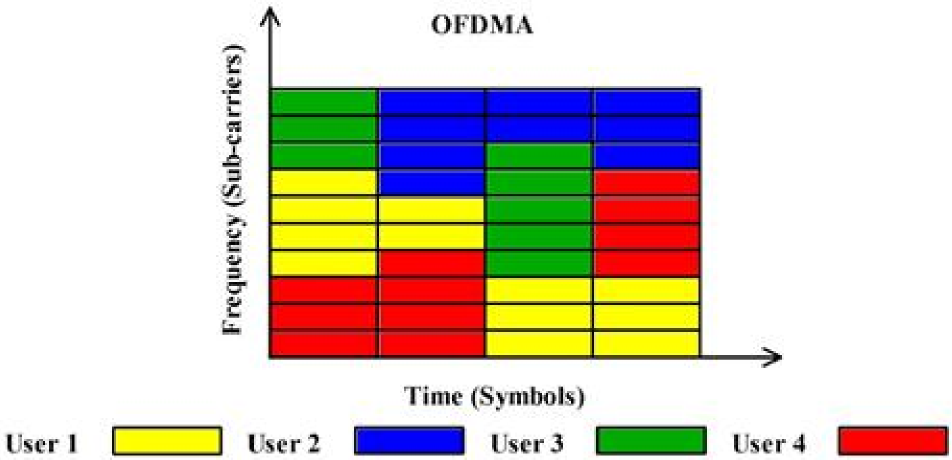

Figure 1: OFDMA dynamic sub-carriers allocation

The sub-carriers mapping schemes is one of the main concerns for LTE as multiple users are assigned by the distributed sub-carriers in OFDMA system [11]. There exist two methods to do sub-carriers mapping: one is the distributed sub-carrier mapping and the other is localized sub-carriers mapping (LOFDMA) scheme [12]. In Distributed sub-carrier mapping scheme, a distributed set of sub-carriers are allocated to users either randomly (Random-Interleaved OFDMA) [13] or at equidistance (Interleaved-OFDMA) [14]. In Localized sub-carrier mapping, every user is allocated a contiguous chunk of band as shown in the Fig. 2. Within an assigned chunk of sub-carriers, no other users are adjusted, but the next user gets the next adjacent chunk of band [15].

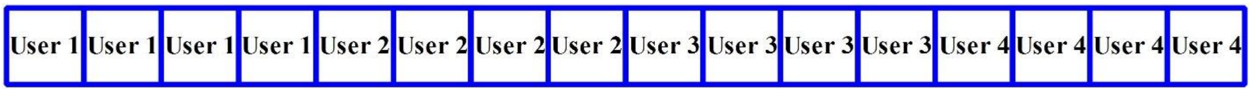

Figure 2: Localized sub-carrier mapping (16 sub-carriers, 4 users, 4 sub-carriers per user)

In the context of resource allocation, sub-carrier mapping schemes are further divided into two types. These are Static sub carrier mapping scheme and Channel Dependent Scheduling (CDS). In a static subcarrier mapping scheme, sub-carrier allocation is pre- defined and remain fixed while in CDS, the sub-carriers are assigned permitting to the channel response for respective user [16]. LOFDMA with CDS shows numerous benefits for its multi-user variety that leads to the enhanced system execution capacity [17]. This is the reason why localized sub-carrier mapping is proposed to be used for the LTE by 3GPP specifications. In LTE, the spacing between sub-carrier is 15 KHz with 66.67 μs OFDMA symbol duration. Fig. 3 shows the conventional FFT-based OFDMA system with sub-carrier mapping scheme. Besides these advantages, Peak to Average Power Ratio (PAPR) values in OFDMA system remains very high and are entitled to in-phase addition of multiple sub-carriers. These high peaks cause high BER ratio at the receiver side [18].

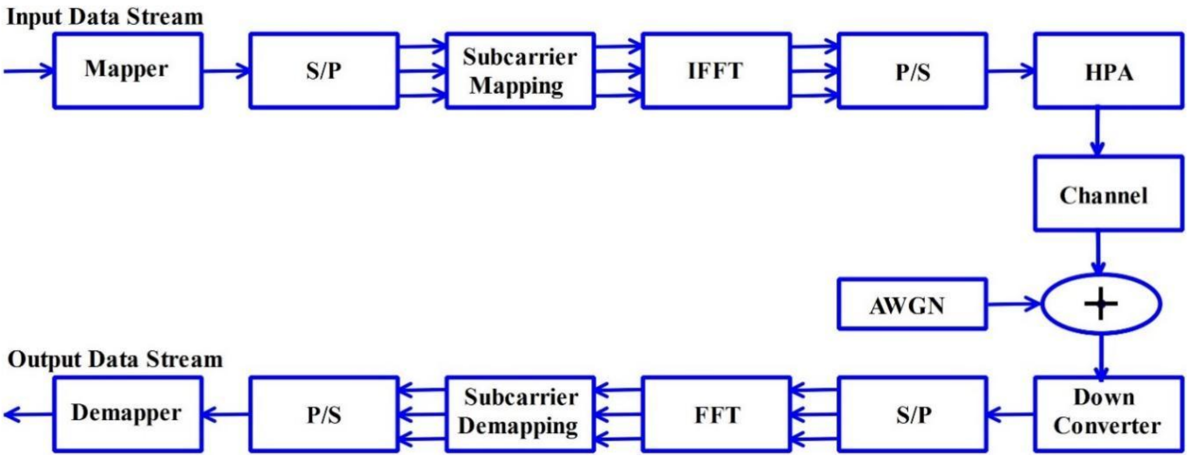

Figure 3: Conventional FFT-based OFDMA system.

The main contributions of this article are summarized below.

We have proposed LWT pre-coding based LOFDMA technique.

The proposed technique is then analyzed and compared with conventional LOFDMA, conventional DWT LOFDMA and FFT pre-coded LOFDMA (SC-FDMA) with the modulation schemes QAM-8, QAM-16 and QAM-64 for PAPR, and BER performance. Furthermore, complexity, bandwidth usage and mode of communication (single or multi-carrier) are some other parameters for which the proposed technique is compared with above mentioned techniques.

The rest of the paper is structured as follows: Section II presents the literature review of the PAPR reduction techniques. We identify the problems in existing works in section III. Section IV explains the framework of our proposed LWT based pre-coded localized

OFDMA technique in detail. Experimental evaluation is done in section V and the results are discussed in section VI. Finally, we conclude the paper in section VII.

Literature Review

Generally, the PAPR reduction techniques available in literature are organized into four major techniques which are 1) Signal Distortion, 2) Signal Scrambling, 3) Coding, and 4) Pre-Coding. Figure 4 portrays the different techniques within these four categories.

The signal distortion technique has a vital role in substantially easing PAPR, never- the less it adds in-band distortion and out-band distortion, leading towards deprivation of Bit BER [19]. Signal Scrambling techniques persuade redundancy but insist on side information, therefore deteriorating the effective throughput of the system [20]. Coding techniques appear as an ideal choice for PAPR reduction due to their endowment of error detection and correction capabilities through variations in coding schemes. Nonetheless, it is notable that these techniques increase system complexity [21], [22]. Likewise, the inclusion of extra bits for code generation adds to bandwidth expansion.

Pre-coding techniques erect out as remarkably effective among the aforesaid schemes, qualified of lowering PAPR to levels similar with single carrier systems [23]. These techniques, depicted by their linearity and simplicity, accomplish PAPR reduction by employing a pre-coding matrix to the constellation signs of the signal preceding to transmission. This tactic not only rationalizes the process, guaranteeing fast transmission, but also re- duces the requirement for side information, thus preserving bandwidth [24]. The common block diagram for pre-coding based PAPR reduction is shown in Fig. 5.

Table 1 gives a general idea of numerous PAPR reduction techniques. The clipping technique, classified as Signal Distortion Technique, possesses minimal complexity. But its integral clipping process produces in-band distortion and out-band contamination, following reduced spectral efficiency and less BER [15]. This destructively affects the complete working of OFDMA systems. In scrambling techniques both Selective Mapping (SLM) and Partial Transmit Sequence (PTS) show superior bandwidth expansion and computational complexity. Particularly, PTS also experiences a data rate deficit. Tone Injection and Tone Reservation techniques are efficient in PAPR reduction but have increased complexity and power consumption. Among both, Tone Injection proves a reasonably lesser data rate loss [13].

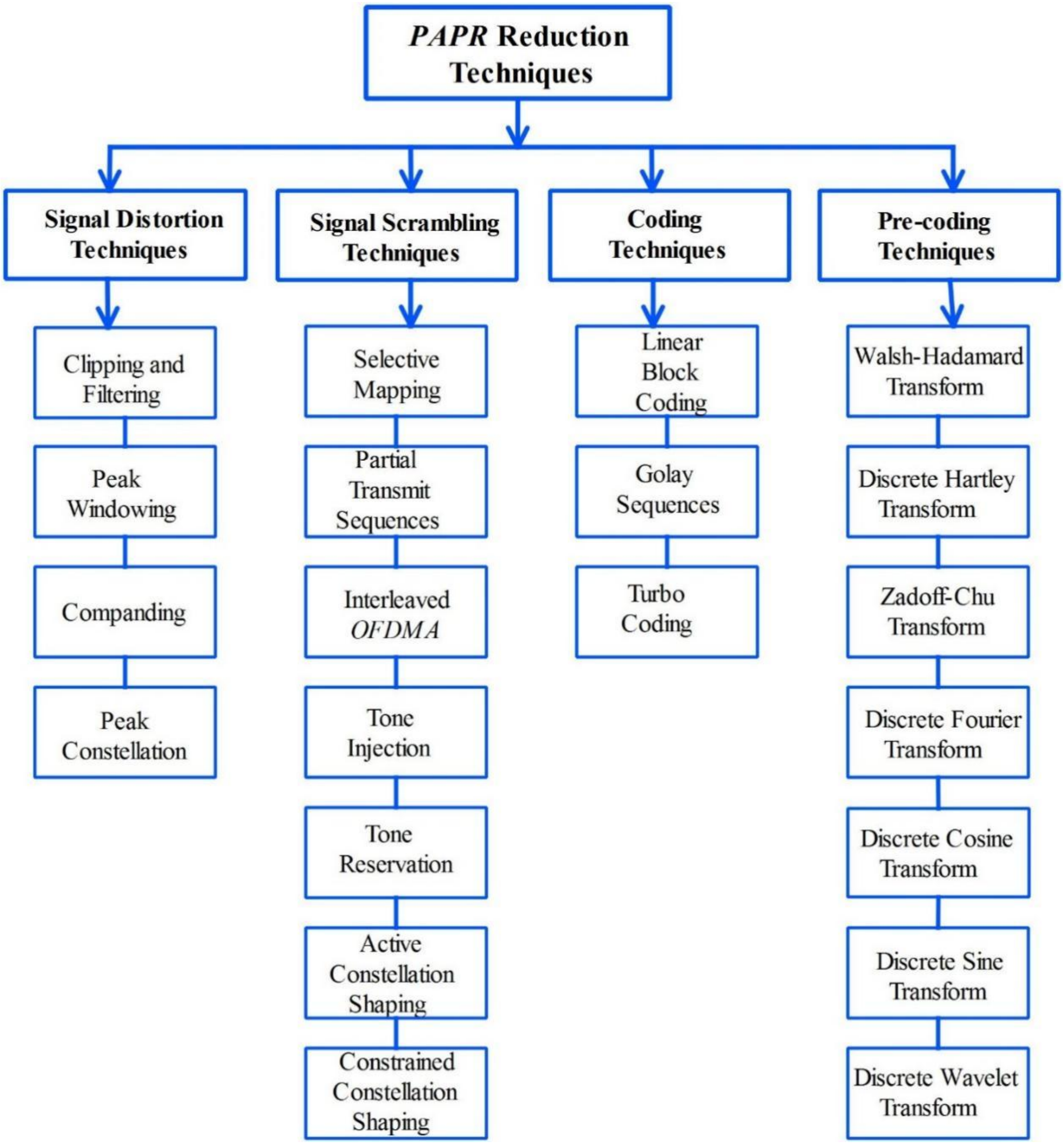

Figure 4: PAPR Reduction Techniques

Pre-coding techniques proved out to be a better technique among the above mentioned techniques, showing superiority in term of BER degradation, complexity, data rate loss, power increase, bandwidth expansion and signal distortion [15]. Moreover, pre-coded OFDMA techniques stand out in PAPR reduction devoid of negotiating the orthogonality among sub carriers [24]. The following section gives an overview of some of the well known pre-coding techniques.

The Walsh-Hadamard Transform (WHT) is an orthogonal linear transform that effectively transforms a binary sequence into orthogonal Wash-Hadamard co-efficients and is

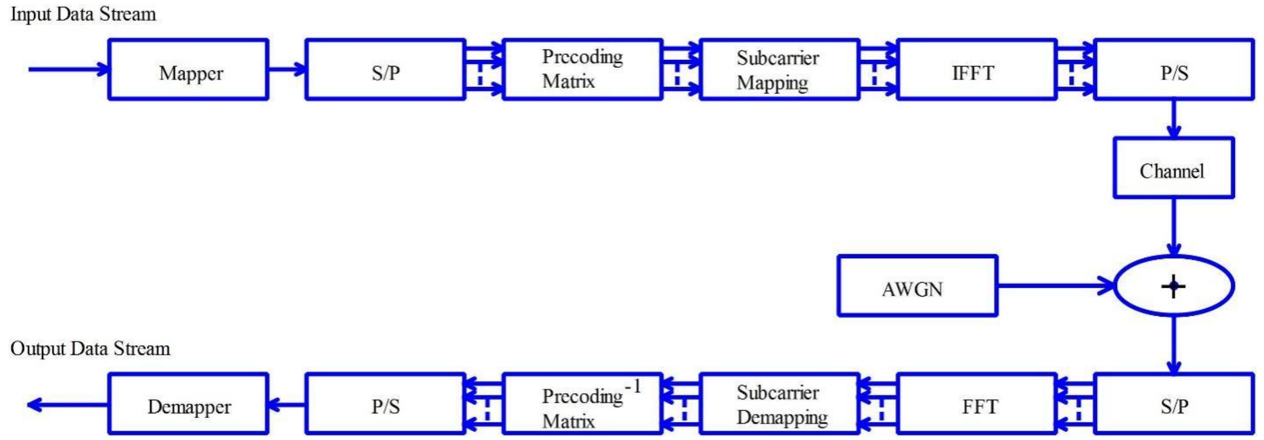

Figure 5: Block diagram of OFDMA technique based om Pre coding

Table 1: ***Comparison of Some Commonly used PAPR Reduction Techniques***

PAPR Reduction Techniques	Complexity	Distortion	BER Degradation	Bandwidth Expansion	Power Increase	Data Rate Loss
Clipping And Filtering	NO	YES	YES	NO	NO	NO
Selective Mapping	YES	NO	NO	YES	NO	NO
Partial Transmit Sequence	YES	NO	NO	YES	NO	YES
Tone Reservation	YES	NO	NO	YES	YES	YES
Tone Injection	YES	NO	NO	YES	YES	NO
Pre-coding Based Techniques	NO	NO	NO	NO	NO	NO

used with butterfly structure [25] [26] [27]. The integration of WHT into a system does not imply substantial complexity [28]. The Discrete Hartley Transform (DHT) is a linear transformation which converts N real numbers represented as $x_0, x_1, \ldots, x_{(N-1)}$ to its corresponding Hartley co-oefficients which are also N real numbers $H_0, H_1, \ldots, H_{(N-1)}$ [29] [30]. The survey demonstrated in [31] show that a DHT pre-coded interleaved-OFDMA technique outruns WHT pre-coding in interleaved-based OFDMA and traditional interleaved-OFDMA. This dominance is ascribed to leveraging the frequency differences contained in the communication channel, indicating a meaningful performance gain, specifically in fading multipath channels [32]. Zadoff-Chu (ZCT) codes denote a specific example of universal Chip-Like polyphase sequences, owning prime correlation domains. Particularly, ZCT sequences having a length of L show a perfect periodic auto- correlation and uphold a persistent degree [33]. In [34], the authors showed a comparison among WHT based STBC MIMO-OFDM, ZCT based STBC MIMO-OFDM and traditional STBC

MIMO-OFDM systems. The outcomes showed that ZCT based STBC MIMO-OFDM performed better than both WHT based STBC MIMO-OFDM and traditional STBC MIMO-OFDM in terms of PAPR reduction. Nevertheless, it is critical to state that the matrix generation method for ZCT is sophisticated, making OFDMA more complex [35]. The dimensions of the Discrete Fourier Transform (DFT) pre-coder are the Inverse Fast Fourier Transform (IFFT) developed to unite dispersed signals [36]. As the inverse transforms, the DFT and IDFT jointly cancel each other, subsequently involving only a single carrier [37]. DFT is utilized as a pre-coding matrix P with dimensions $L \times L$ prior to implementing the IFFT. This alleviate the PARP of the system [38]. The authors in [32] determined that, among the reviewed pre-coding methods, DFT sets out as the best applicable in PAPR reduction, complexity and BER performance. A further advantage is that it doesn't need any exceptional hardware for execution. Conversely, it changes the system into a single-carrier system, indicating its primary drawback. The Discrete Cosine Transform (DCT) is a method that corresponds to a limited sequence of data in the form of cosine functions swinging at diverse frequencies. Similar to the DFT, the DCT sorts out real numbers utterly [39]. Remarkably, DCTs function on real data with even symmetry, making them different from DFTs. One crucial difference lies in the lengths of DFTs, which are almost twice the length of DCTs [40] [41]. In am experiment shown by the author in [42], it was detected that DCT-based OFDM and DFT-based OFDM show approximately matching results in terms of BER performance over the AWGN channel. Especially, the DCT, being a real transform, establishes better computational efficiency than the fundamental complex DFT. Moreover, research reported in [43] reveals that DCT-OFDM outstrips DFT-OFDM in characteristics such as BER performance, PAPR, computational complexity. The operation of the Discrete Sine Transform (DST) reflects that of the DCT. They are, to some level, converses of each other, with differences in DST and DCT differing on boundary conditions [44]. In the DST matrix, every single factor is required to have equivalent magnitude, and the matrix should be non-singular [45]. Both DST and DCT bring forth similar results in aspects of PAPR reduction. Yet, the selection between cosine and sine functions can be critical in specific applications. For example, in compression, cosine functions are frequently chosen due to their remarkable efficiency, involving less functions to estimate a standard signal [46]. The Discrete Wavelet Trans- form (DWT) yields discrete outputs afterwards employed to discrete datasets [47] finally converting the data to the wavelet domain. In numerous DSP functions, identifying the frequency contents of a signal is significant. Amongst numerous transforms, Wavelet Transform sets out to deliver an excellent time-frequency interpretation of the signal [48].

Problem Statement

PAPR is one of the major problems in multicarrier communication systems like OFDMA. When the sub-carriers which are independently modulated add up coherently, lead to an instantaneous power exceeding the average power level. So, the ratio of the peak power value to the average power value is termed as PAPR which is given by [14].

$$PAPR\ (x[n]) = \max_{0\le n\le N-1} \frac{|x[n]|^2}{E[|x[n]|^2]}, \qquad (1)$$

Raised PAPR levels push High Power Amplifiers (HPA) into a non-linear performing zone, bringing in-band distortion and out-of-band radiation, as stated in [19] and [20]. The in-band distortion poorly influences BER execution, however out-of-band radiation manages to interference problems with neighboring channels. The consequences range to the effectiveness of HPAs, obfuscating the Digital-to-Analog and Analog-to-Digital converters within transmitters. The passing of high-peak signals via non-linear HPAs expand spectral broadening, consequently encouraging the vibrant range of DAC and raising the whole system cost [9].

To avoid HPA from going into the non-linear region, one method is to reduce the average power of the signal. Conversely, this approach comes at the cost of reducing the Signal-to-Noise Ratio (SNR) and consequently negotiating the BER performance, as indicated in [12]. On the other hand, utilizing amplifiers through large linear regions is a choice, but the high expenses linked with such amplifiers can increase the whole transmitter expenses [47]. Subsequently, to tackle the task of high PAPR, it becomes necessary to concentrate on decreasing the peak power of the signal.

The higher PAPR values linked with OFDMA have stimulated the approval of precise tactics in Long LTE-A. In the downlink, LTE-A uses OFDMA, whereas the uplink transmission goes for Single Carrier OFDMA (SC-FDMA). SC-FDMA exercises a procedure where the data is allocated across all sub-carriers before experiencing IFFT, leading to a reduced variation in the instantaneous power of the transmitted signal. Figure 6 demonstrates a proportional illustration of OFDMA and SC-FDMA.

The reduction in PAPR, i.e. the expected results of this research work, will help in linearizing the non-linear amplification by confining the OFDMA symbols within the lin- ear range of power amplifiers. Hence, the existing expensive and inefficient transmitters and receivers can be replaced by the economical and efficient transmitters and receivers. So, the expected results of this work can be utilized in designing the cost-effective com- munication system

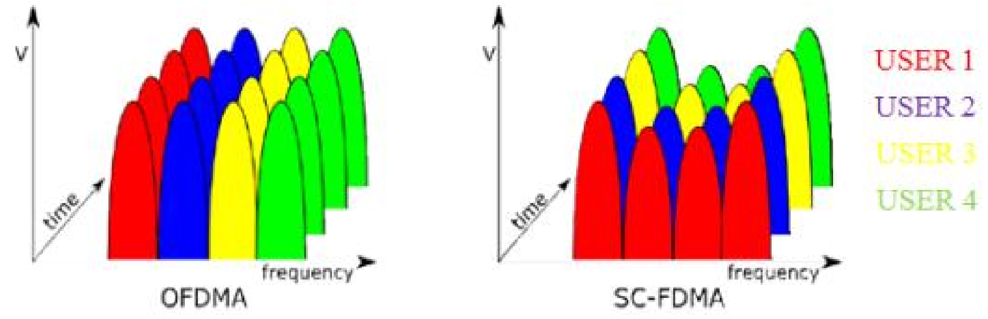

Figure 6: OFDMA vs SC-FDMA comparison

Proposed Technique

The proposed LWT pre-coding based Localized OFDMA system is shown in the Fig. 7. The binary information data, represented as X experiences grouping and later mapped via digital modulation techniques such as 8-QAM, 16-QAM, or 64-QAM. Succeeding the mapping procedure, the data is pointed through a Serial to Parallel converter, producing a complex vector of size L. This vector can be denoted in matrix form as:

$$\overline{X} = [x_0 \quad x_1 \quad \cdots \quad x_{L-1}]^T \tag{2}$$

$$P = \begin{bmatrix} p_{0,0} & p_{0,1} & \cdots & p_{0,L-1} \\ p_{1,0} & p_{1,1} & \cdots & p_{1,L-1} \\ \vdots & \vdots & \ddots & \vdots \\ p_{L-1,0} & p_{L-1,1} & \cdots & p_{L-1,L-1} \end{bmatrix} \tag{3}$$

After S/P conversion, a LWT pre-coding matrix of size $L{\times}L$ is applied to the L distinct input data set or constellation points. The LWT pre-coding matrix can be represented as:

$$\overline{Y_P} = P.\overline{X} = \begin{bmatrix} p_{0,0} & p_{0,1} & \cdots & p_{0,L-1} \\ p_{1,0} & p_{1,1} & \cdots & p_{1,L-1} \\ \vdots & \vdots & \ddots & \vdots \\ p_{L-1,0} & p_{L-1,1} & \cdots & p_{L-1,L-1} \end{bmatrix} \begin{bmatrix} x_0 \\ x_1 \\ \vdots \\ x_{L-1} \end{bmatrix}$$

$$= [p_0 x_0 \quad p_1 x_1 \quad \cdots \quad p_{L-1} x_{L-1}]^T \tag{4}$$

This pre-coding matrix of size $L \times L$ is multiplied with the input data matrix of size $L \times 1$ to give the output matrix of size $L \times 1$, which can be represented as:

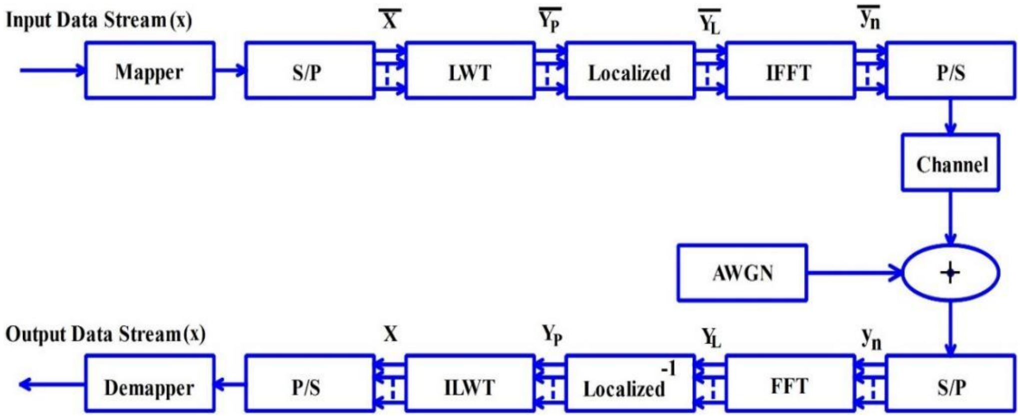

Figure 7: Proposed LWT pre-coding based localized OFDMA system

$$\overline{Y_P} = P.\overline{X} = \begin{bmatrix} p_{0,0} & p_{0,1} & \cdots & p_{0,L-1} \\ p_{1,0} & p_{1,1} & \cdots & p_{1,L-1} \\ \vdots & \vdots & \ddots & \vdots \\ p_{L-1,0} & p_{L-1,1} & \cdots & p_{L-1,L-1} \end{bmatrix} \begin{bmatrix} x_0 \\ x_1 \\ \vdots \\ x_{L-1} \end{bmatrix}$$

$$= [p_0x_0 \quad p_1x_1 \quad \cdots \quad p_{L-1}x_{L-1}]^T \qquad (5)$$

This matrix can be written as:

$$\overline{Y_P} = \sum_{m=0}^{L-1} \sum_{l=0}^{L-1} P_{m,l} \, . \, X_m \qquad (6)$$

Where $P_{m,l}$ shows the element of the pre-coding matrix P at the m^{th} row and the l^{th} column. $\overline{Y}P$ is the output from the pre-coder (LWT). After pre-coding matrix step, the Localized sub-carrier mapping scheme is applied which is given by:

$$\overline{Y_L} = \begin{cases} \overline{Y_q} & 0 \le q \le M-1 \\ 0 & M \le q \le N-1 \end{cases} \qquad (7)$$

Now the value of n is given by: $n = Q \times m + q$ Where $0 \le q \le Q-1$, $0 \le m \le M-1$ and

$$Q = \frac{\text{No. of subcarriers (L)}}{\text{Data block size (M)}} \qquad (8)$$

IFFT is applied to the output of the localized scheme block. Now, the complex baseband LWT pre-coded LOFDMA signal with L sub-carriers can be written as:

$$\overline{y_n} = \text{IFFT}\{\overline{Y_L}\} = \frac{1}{\sqrt{L}} \sum_{m=0}^{L-1} \overline{Y_L} \, . \, e^{j2\pi\frac{n}{L}k} \quad n = 0,1,2, \ldots . L-1 \quad (9)$$

Putting $n = Q \times m + q$ and $L = Q \times M$ in (9) gives:

$$\overline{y_n} = \frac{1}{\sqrt{Q \times M}} \sum_{m=0}^{L-1} \overline{Y_L} \, . \, e^{j2\pi\frac{Q\times m+q}{Q\times M}k}$$

$$= \frac{1}{\sqrt{Q\times M}} \sum_{m=0}^{M-1} \overline{Y_P} \, . \, e^{j2\pi\frac{m}{M}k} \qquad M \qquad (10)$$

The PAPR of the signal $\overline{y_n}$ obtained after IFFT block can now be calculated as:

$$PAPR\ (\overline{y_n}) = \max_{0 \le n \le L-1} \frac{[|\overline{y_n}|^2]}{E[|\overline{y_n}|^2]} \qquad (11)$$

The data is now converted from parallel to serial and sent through the channel towards the receiver.

Simulation Setup

We used Matlab 2021b for conducting extensive simulations. The flow diagram shown in Fig. 8 explains the complete simulation process. First of all the random data is generated and the simulation parameters are set. After that a modulation technique is chosen and then that data is converted from serial to parallel and localized sub carrier mapping scheme is applied to the parallel data. A pre-coding matrix is selected (if applicable) and the PAPR is calculated for the respected pre-coding matrix as the PAPR is observed on transmitter before applying the channel parameters. Similarly, on the receiver side the channel parameters are removed accordingly and followed by the inverse pre-coding step. Again data is converted from parallel to serial and delocalized sub-carrier mapping is done. After that the demodulation is done and the Bit Error Rate is calculated for the data received at the receiver side. The simulation parameters for finding PAPR are listed below in the Table 2 the simulation parameters for the calculation of BER are listed in the Table 3.

Results

PAPR Results

The PAPR is calculated through Complementary Cumulative Distributive Function (CCDF). It analyzes the power peaks of a signal. CCDF is actually the probability that PAPR will be greater than a specific value, sometimes called clipping value ($PAPR_0$) and it is found from the Cumulative Distributive Function (CDF) which is the probability that PAPR will be less than or equal to $PAPR_0$ and is given as:

$$CDF = P(PAPR \leq PAPR_0) \tag{12}$$

Where P denotes probability and $PAPR_0$ is any specified value of PAPR. As the total probability is equal to unity, the CCDF is calculated as:

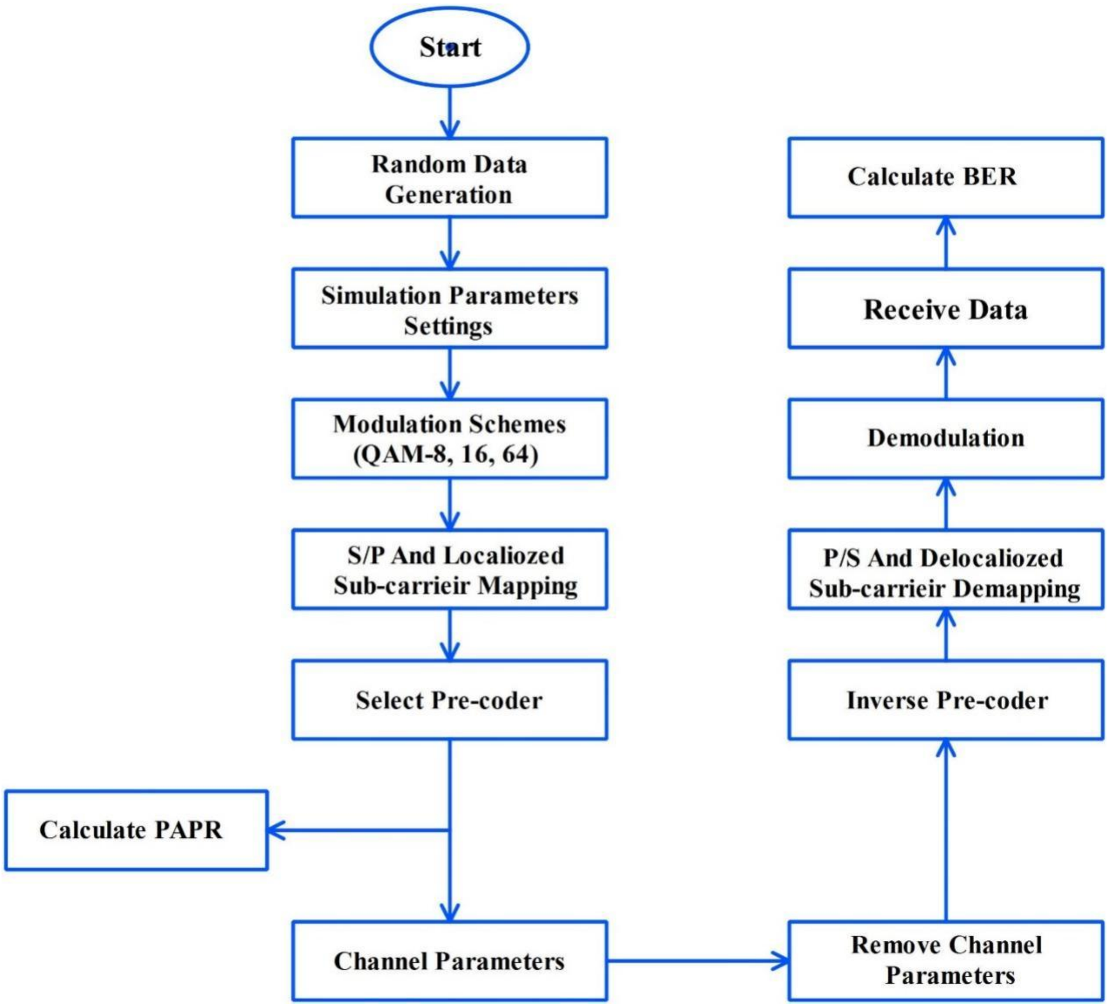

Figure 8: Flow diagram for simulation

$$P(PAPR > PAPR_0) = 1 - CDF$$
$$= 1 - P(PAPR \leq PAPR_0) \tag{13}$$

Based on the parameters given in the Table 2 the simulation results are obtained which are explained in the Fig. 9 to Fig. 11 The PAPR values are compared for conventional LOFDMA [15], DWT-LOFDMA [49], FFT LOFDMA [37] and the proposed LWT based pre-coded LOFDMA.

In Fig. 9, it is shown that the LWT pre-coded based LOFDMA system gives best result as compared to the conventional LOFDMA and conventional DWT-LOFDMA using QAM-8 modulation scheme. However, it is also shown that the FFT pre-coded based LOFDMA system gives good performance than LWT pre-coded LOFDMA system as it has no effect after 6 dB of PAPR. It can be seen that the conventional LOFDMA has the worst result of all as still the probability of PAPR exists beyond 8dB. Both conventional DWT-LOFDMA and LWT pre-coded based LOFDMA have maximum 8dB of PAPR. Both have the same ending point, but as can be seen that the LWT pre-coded LOFDMA has a lowest probabilities between 3.7dB to 7.7dB.

Table 2: ***Simulation Parameters for PAPR Analysis***

Simulation Parameters For PAPR		
Parameters	**LOFDMA**	**Proposed LOFDMA**
Frequency	10MHz	10MHz
No. of Runs	1000	1000
Modulation Schemes	QAM-8 QAM-16 QAM-64	QAM-8 QAM-16 QAM-64
IFFT Size	512	512
No. of Sub-carriers	64	64
Sub-carrier Mapping Scheme	Localized	Localized
Localized Interval	4	4
Cyclic Prefix	12.5 %	No Need
Pre-coders	FFT	LWT
Type of Channel	Rayleigh Fading	Rayleigh Fading
Symbol Length	1×10^3	1×10^3
SNR Range	1:20	1:20

Fig. 10 shows the results for modulation scheme QAM-16. It is revealed that at first the LWT pre-coded based LOFDMA system gives worst result as compared to the conventional DWT LOFDMA but after crossing 6dB, the LWT pre-coded LOFDMA has a best result than conventional DWT LOFDMA and conventional LOFDMA techniques. For QAM-16, both LWT pre-coded LOFDMA and conventional DWT LOFDMA has no effect after 7dB. But here the probability at this point for LWT pre-coded LOFDMA is much decreased compared to QAM-8 graph. On the other hand, Conventional DWT LOFDMA has not much effect on probability at this point (7dB). Conventional LOFDMA has still the worst result among all the techniques as its effect exists after the 8dB.

Table 3: ***Simulation Parameters for BER Analysis***

Simulation Parameters For BER		
Parameters	**LOFDMA**	**Proposed LOFDMA**
Frequency	10MHz	10MHz
No. of Runs	1000	1000
Modulation Schemes	QAM-8 QAM-16 QAM-64	QAM-8 QAM-16 QAM-64
IFFT Size	512	512
FFT Size	512	512
No. of Sub-carriers	64	64
Sub-carrier Mapping Scheme	Localized	Localized
Localized Interval	4	4
Cyclic Prefix	12.5 %	No Need
Pre-coders	FFT	LWT
Type of Channel	Rayleigh Fading	Rayleigh Fading
Symbol Length	1×10^3	1×10^3
SNR Range	1:20	1:20
Equalization	MMSE	MMSE

However, it can also be seen that the FFT pre-coded based LOFDMA system gives good performance than LWT pre-coded based LOFDMA system, as it has again no effect after 6dB. But in case of QAM-16, its probability has increased.

Fig. 11 shows the results for PAPR for the modulation scheme QAM-64. It is revealed that conventional DWT LOFDMA has a worst result than both the conventional LOFDMA and LWT pre-coded LOFDMA, but after 7dB it becomes even better than LWD pre-coded LOFDMA technique. But LWT pre-coded LOFDMA has no effect after 7dB while conventional DWT LOFDMA has PAPR values even after 8dB. FFT pre-coded LOFDMA has still better result among all the techniques mentioned above but this time its

PAPR reach to 7dB from 6dB in QAM-8 and QM-16. The LWT pre-coded LOFDMA has no effect after 7dB as was for QAM-16 but its probability has increased.

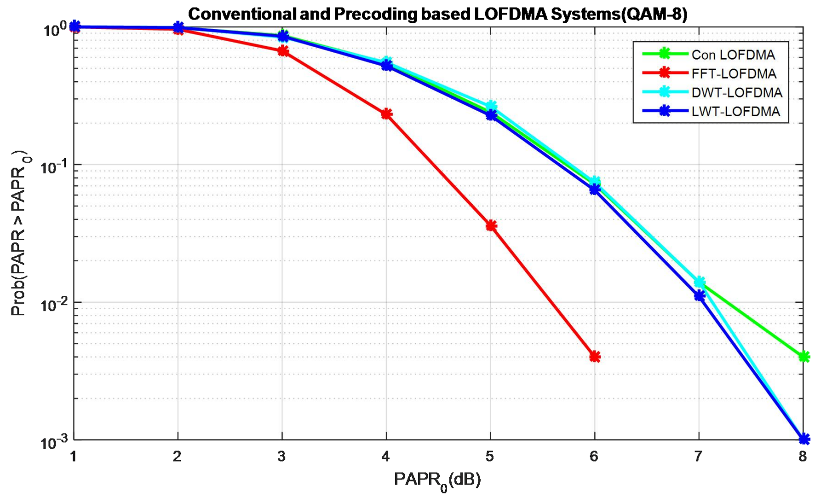

Figure 9: PAPR result comparison using QAM-8.

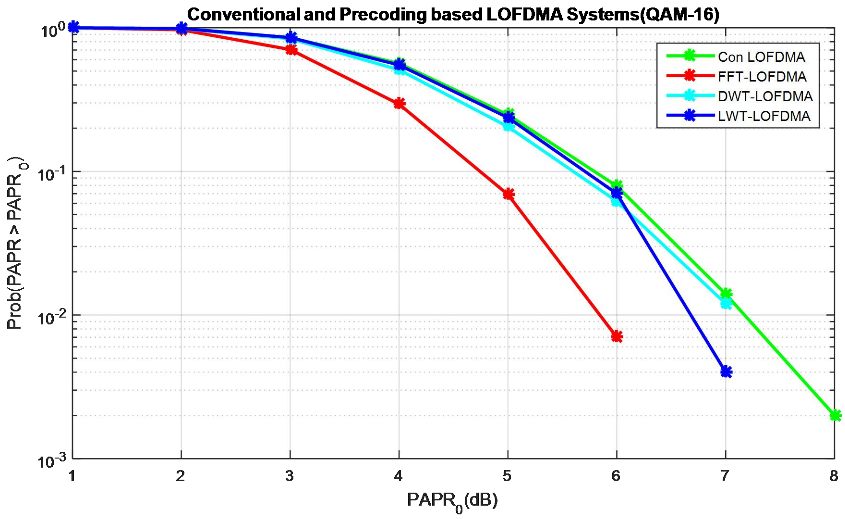

Figure 10: PAPR result comparison using QAM-16.

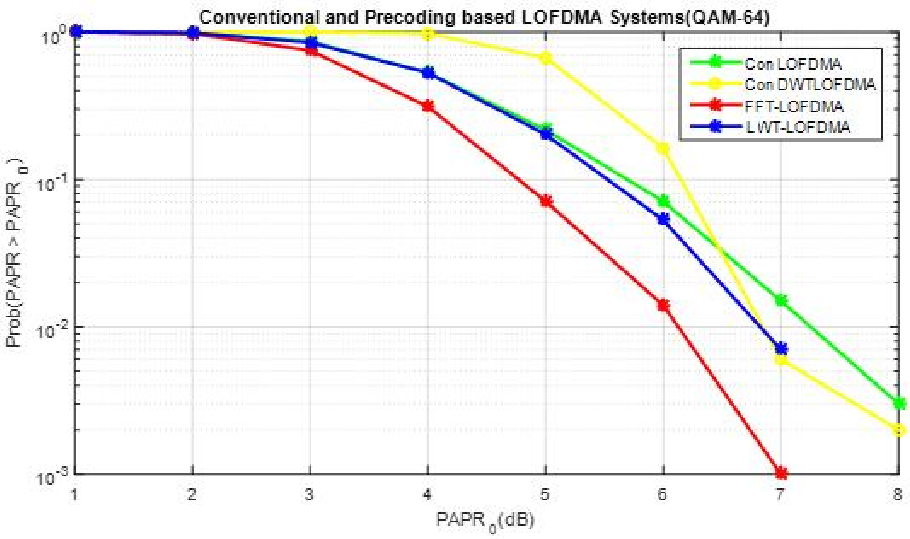

Figure 11: PAPR result comparison using QAM-64.

BER Results

BER is defined as the ratio of number of bits in error to the total number of transmitted bits, processed or received over a given period of time. It actually gives the rate at which the error occurs in communication system. This statement can be easily represented by the formula:

$$BER = \frac{No.\,of\ bits\ in\ error}{Total\ No.\,of\ bits\ transmitted} \tag{14}$$

BER performance is evaluated for different techniques from the graph of BER vs Eb/N0 as shown in the Fig. 12 to Fig. 14. Eb/N0 is the ratio of energy per bit (Eb) and Noise Spectral Density (N0), i.e. the noise power per unit bandwidth. It is the Signal-to-Noise Ratio (SNR) for digital communication systems. It is a dimensionless ratio expressed in dB.

Fig. 12 shows the BER curves for the modulation scheme QAM-8. It is shown that the LWT pre-coded LOFDMA gives the best result among all the techniques using QAM-8 modulation scheme. Both LWT pre-coded LOFDMA and conventional LOFDMA has the maximum of Eb/N0 as 13.6dB, but LWT pre-coded LOFDMA has the lowest BER at this point. FFT pre-coded *LOFDMA* and conventional DWT LOFDMA has the maximum of Eb/N0 as 16dB. BER of all the techniques at Eb/N0 = 13.6dB is: LWT pre-coded LOFDMA = 0.0014, Conventional DWT LOFDMA = 0.0027, Conventional LOFDMA = 0.0042 and FFT pre-coded LOFDMA = 0.005. Hence the LWT pre-coded LOFDMA has the lowest value of BER for the same value of Eb/N0.

Fig. 13 shows the comparison of BER vs Eb/N0 graphs for the modulation scheme QAM-16. It is shown that the all the techniques have a maximum value of Eb/N0 at 16dB. BER of all the techniques at Eb/N0 = 16dB is: LWT pre-coded LOFDMA = 0.0018, Conventional DWT LOFDMA = 0.00225, Conventional LOFDMA = 0.00225 and FFT pre-coded LOFDMA = 0.003. Hence the LWT pre-coded LOFDMA has the lowest value of BER for the same value of Eb/N0.

Fig. 14 shows the comparison of BER vs Eb/N0 graphs for the modulation scheme QAM-64. It is shown that the all the techniques have a maximum value of Eb/N0 at 23.5dB. BER of LWT pre-coded LOFDMA at Eb/N0 = 23.5dB is 0.000175. Conventional DWT LOFDMA, Conventional LOFDMA and FFT pre-coded LOFDMA have the same value of BER of 0.0005 as they end at the same point. Hence for the same value of Eb/N0, the LWT pre-coded LOFDMA has the lowest value of BER.

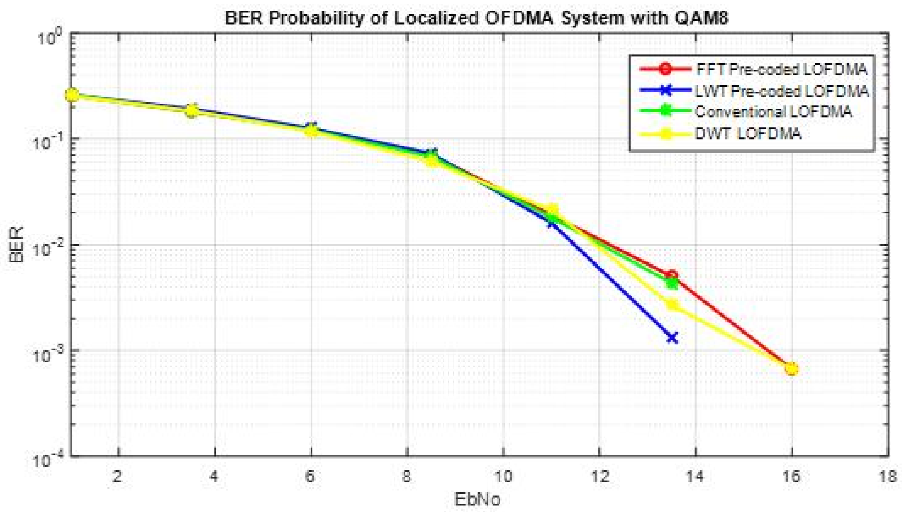

Figure 12: BER vs Eb/N0 comparison for QAM-8 modulation scheme.

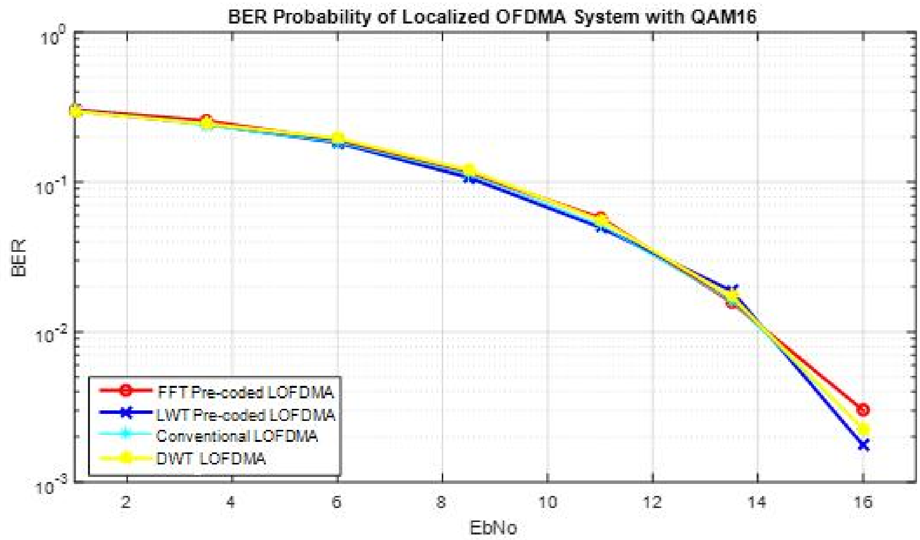

Figure 13: BER vs Eb/N0 comparison for QAM-16 modulation scheme.

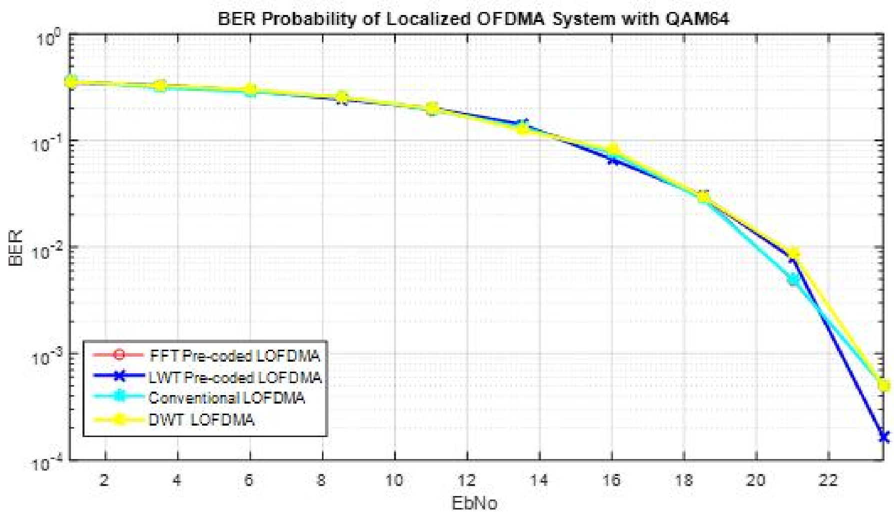

Figure 14: BER vs Eb/N0 comparison for QAM-64 modulation scheme.

Summary of Results Obtained From PAPR and BER

The results obtained for PAPR for different techniques are summarized in the Table 4 for their maximum values of PAPR.

It is observed from the summary Table 4 that for the modulation schemes QAM-8, QAM-16 and QAM-64, the PAPR value of conventional LOFDMA can exceed 8dB. For all the modulation schemes mentioned above, FFT pre-coded LOFDMA has the best result regarding the PAPR value among all the techniques mentioned in the Table 4. Both Conventional DWT LOFDMA and LWT pre-coded LOFDMA seems to be same for the modulation schemes QAM-8 and QAM-16. In case of QAM-8, both techniques have the same probabilities at the ending point but for the PAPR values from 3.7dB to 7.7dB, LWT pre-coded LOFDMA has less probability than conventional DWT LOFDMA. On the other hand, in case of QAM-16, the maximum PAPR values are same but from the Fig. 10, it can be shown that LWT pre-coded LOFDMA has less probability at this point than conventional DWT LOFDMA.

Similarly, the results obtained for BER vs Eb/N0 for different techniques are summarized in the Table 5 for some specific values of Eb/N0. In all cases for modulation schemes QAM-8, QAM-6 and QAM-64 respectively, the LWT pre-coded LOFDMA has the best result compared to all the above mentioned techniques in Table 5.

Table 4: ***Summary of Results For PAPR***

Summary of Results for PAPR			
Technique	**PAPR Value**		
	QAM-8	**QAM-16**	**QAM-64**
Conventional LOFDMA	Beyond 8 dB	Beyond 8 dB	Beyond 8 dB
FFT Pre-coded LOFDMA	6 dB	6 dB	7 dB
Conventional DWT LOFDMA	8 dB	7 dB	Beyond 8 dB
LWT Pre-coded LOFDMA	8 dB	7 dB	7 dB

Table 5: Summary of Results for BER vs Eb/N0

Summary of Results for BER vs Eb/N_0			
Technique	**BER Value**		
	QAM-8 At Eb/N_0 = (13.6dB)	**QAM-16 At Eb/N_0 = 16dB**	**QAM-64 At Eb/N_0 = 23.5dB**
FFT Pre-coded LOFDMA	0.005	0.003	0.0005
Conventional LOFDMA	0.0042	0.00225	0.0005
Conventional DWT LOFDMA	0.0027	0.00225	0.0005
LWT Pre-coded LOFDMA	0.0014	0.0018	0.000175

Comparison of Complexity, Bandwidth Expansion and Multi- carrier Communication

The complexity, bandwidth usage and multi-carrier communication is compared in the Table 6 for Conventional LOFDMA, Conventional DWT LOFDMA, LWT pre-coded LOFDMA and FFT pre-coded LOFDMA techniques.

Complexity is defined as the number of complex multiplications involved in processing each frame of data. For N-point FFT the computational complexity is $O(N\log_2 N)$. For the FFT pre-coded LOFDMA where one extra block of FFT is also included before the IFFT block, then its computational complexity gets doubled than the conventional FFT based LOFDMA. As discussed in [40], the lifting scheme asymptotically reduces the computational complexity of standard wavelet transform by factor of two. So, as the computational complexity of DWT is $O(N)$, then the computational complexity of LWT is $O(N/2)$. Therefore, the computational complexity of LWT Pre-coded LOFDMA, due to one additional block of IFFT is $O\left(\frac{N}{2}\right) + O(N\log_2 N)$. Thus, the proposed technique has a less computational complexity than the FFT pre-coding based LOFDMA while it has a minor compromise on the computational complexity compared to Conventional DWT based LOFDMA and Conventional LOFDMA techniques.

As wavelet transform do not need any cyclic prefix, so they do not expand the bandwidth of the system. Hence there is no bandwidth expansion due to Conventional DWT LOFDMA and LWT Pre-coded LOFDMA techniques. Furthermore, Conventional LOFDMA, Conventional DWT LOFDMA and LWT pre-coded LOFDMA ensures the multi-carrier communication while on the other hand FFT pre-coded LOFDMA is a sin- gle carrier communication (SC-LOFDMA) as the IFFT and FFT blocks cancels the effect of each other.

Table 6: Comparison of complexity, bandwidth usage and multi-carrier communication

Comparison of Complexity, Bandwidth Expansion and Multi-carrier Communication			
Technique	**Computational Complexity**	**Bandwidth Expansion**	**Multi-carrier**
Conventional LOFDMA	$O(N\log_2 N)$	YES	YES
FFT Pre-coded LOFDMA	$2 \times O(N\log_2 N)$	YES	NO
Conventional DWT LOFDMA	$O(N)$	NO	YES
LWT Pre-coded LOFDMA	$O(N/2) + O(N\log_2 N)$	NO	YES

1 Conclusion

In this paper, LWT pre-coding based LOFDMA technique has been presented. The proposed technique is analyzed and compared with Conventional LOFDMA, Conventional DWT LOFDMA and FFT pre-coded LOFDMA (SC-FDMA) with the modulation schemes QAM-8, QAM-16 and QAM-64 for PAPR, and BER. Furthermore, complexity, bandwidth usage and mode of communication (single or multi-carrier) are some other parameters for which the proposed technique is compared with above mentioned techniques. From the results and discussions, it is concluded that LWT pre-coded LOFDMA has the best result for PAPR among all techniques analyzed in this thesis except the FFT pre- coded LOFDMA but the main limitation of FFT pre-coded LOFDMA is that it makes the system a single carrier system. Moreover, it has more complexity as compare to LWT pre-coded LOFDMA technique. On the other hand, LWT pre-coded LOFDMA is a multi-carrier communication technique.

It is also concluded from BER results that LWT pre-coded LOFDMA has the lowest BER values among all the techniques for all modulation schemes. If focused on the PAPR performance of FFT Pre-coded LOFDMA system, it is best from LWT Pre-coded LOFDMA technique, but the BER performance is still less as compare to LWT pre-coded LOFDMA technique. This is because the FFT Pre-coded LOFDMA technique destroys the orthogonality of the subcarriers which causes ISI at the receiver side. Moreover, LWT Pre-coded LOFDMA has the lowest computational complexity and does not expands the bandwidth of the system as it does not require the cyclic prefix.

References

[1] H. A. M. Ramli, A. H. A. Hashim, and A. L. Asnawi, "Effective scheduling mechanism for a mixture of 5g multimedia use cases," *Computers and Electrical Engineering*, vol. 108, p. 108701, 2023.

[2] M. J. Alam, M. R. Hossain, S. Azad, and R. Chugh, "An overview of lte/lte-a heterogeneous networks for 5g and beyond," *Transactions on Emerging Telecommunications Technologies*, p. e4806, 2023.

[3] R. T. Ahmed and O. Q. J. AL-Thahab, "Comprehensive review on lte-ber reduction with modern transform," *2022 3rd Information Technology To Enhance e-learning and Other Application (IT-ELA)*, pp. 116–122, 2022.

[4] H. Harkat, P. Monteiro, A. Gameiro, F. Guiomar, and H. Farhana Thariq Ahmed, "A survey on mimo-ofdm systems: review of recent trends," *Signals*, vol. 3, no. 2, pp. 359–395, 2022.

[5] E. Mozaffariahrar, F. Theoleyre, and M. Menth, "A survey of wi-fi 6: Technologies, advances, and challenges," *Future Internet*, vol. 14, no. 10, p. 293, 2022.

[6] S. Li, N. Zhang, H. Chen, S. Lin, and H. Wu, "Joint subcarrier allocation, modulation mode selection, and trajectory design in a uav-based ofdma network," *IEEE Communications Letters*, vol. 26, no. 9, pp. 2111–2115, 2022.

[7] W. Guo, N. M. F. Qureshi, I. F. Siddiqui, and D. R. Shin, “Cooperative communi- cation resource allocation strategies for 5g and beyond networks: A review of archi- tecture, challenges and opportunities,” *Journal of King Saud University-Computer and Information Sciences*, vol. 34, no. 10, pp. 8054–8078, 2022.

[8] X. Tan, L. Zhou, H. Wang, Y. Sun, H. Zhao, B.-C. Seet, J. Wei, and V. C. Leung, “Co- operative multi-agent reinforcement-learning-based distributed dynamic spectrum access in cognitive radio networks,” *IEEE Internet of Things Journal*, vol. 9, no. 19,

pp. 19477–19488, 2022.

[9] F. Aouissi, “Evaluation d’un syst`eme mimo-noma de communication sans fil 5g,” 2022.

[10] F. B. Muslim, M. Hussain, U. Hashmi, A. Aneesullah, M. Aamir, and A. Zahir, “Performance evaluation of a multicarrier mimo system based on dft-precoding and subcarrier mapping,” *Facta Universitatis, Series: Electronics and Energetics*, vol. 35, no. 2, pp. 253–268, 2022.

[11] V. Venkataramanan, R. K. Dehiya, A. Vora, A. Shah, A. Nafre, and G. Prachi, “Lte modulation and coding schemes for 6g networks,” *International Journal of Sensors Wireless Communications and Control*, vol. 12, no. 4, pp. 326–332, 2022.

[12] W. Jin, M. Wang, G. Yang, and Z. Chen, “Energy-efficient and fading-resistant multi- mode ofdm-im with high dimensional mapping,” *IEEE Transactions on Wireless Communications*, 2022.

[13] M. Y. El-Ganiny, A. A. Khalaf, A. I. Hussein, and H. F. Hamed, “Hybrid papr reduction schemes for different ofdm-based vlc systems,” *Opto-Electronics Review*, vol. 30, no. 3, 2022.

[14] R. Jaikumar, M. Mukunthan, C. Arvind, R. Lavanya, and K. Srihari, “A low com- plexity spatial mapping assisted companding scheme (smacs) for papr minimization in ofdm systems,” *National Academy Science Letters*, vol. 45, no. 6, pp. 511–515, 2022.

[15] A. Tiwari, V. T. Mustaqueemuddin, S. Siddharth, and V. Gupta, “Comparison of different techniques of papr reduction schemes of ofdm system,” in *IPEC*, vol. 1,

p. 02, 2022.

[16] L. R. Nair, S. S. Pillai, and G. Shiny, “Lfdma papr minimization using advanced selective mapping-based phase factor optimization,” in *2022 IEEE 19th India Council International Conference (INDICON)*, pp. 1–7, IEEE, 2022.

[17] S. Feng, Q. Wu, C. Dong, and B. Li, “A spectrum enhanced aco-ofdm scheme for opti- cal wireless communications,” *IEEE Communications Letters*, vol. 27, no. 2, pp. 581– 585, 2022.

[18] J. Arun Prem Santh, D. Judson, K. Selvaraj, and V. Bhaskar, “Improved papr reduc- tion using gamma correction in sc-fdma systems under multipath fading channels,” *Wireless*

Personal Communications, vol. 125, no. 3, pp. 2889–2905, 2022.

[19] A. Hussein, M. Y. El-Ganiny, H. F. Hamed, and A. A. Khalaf, "Hybrid papr reduction schemes for different ofdm-based vlc systems," 2023.

[20] V. S. Nagaraju, R. Anusha, and R. R. Vallabhuni, "A hybrid papr reduction technique in ofdm systems," in *2020 IEEE International Women in Engineering (WIE) Conference on Electrical and Computer Engineering (WIECON-ECE)*, pp. 364–367, IEEE, 2020.

[21] S. Sarowa, N. Kumar, S. Agrawal, and B. S. Sohi, "Evolution of papr reduction techniques: A wavelet based ofdm approach," *Wireless Personal Communications*, vol. 115, no. 2, pp. 1565–1588, 2020.

[22] S. Mohammady, R. Farrell, D. Malone, and J. Dooley, "Performance investigation of peak shrinking and interpolating the papr reduction technique for lte-advance and 5g signals," *Information*, vol. 11, no. 1, p. 20, 2019.

[23] B. Bakkas, R. Benkhouya, I. Chana, and H. Ben-Azza, "Palm date leaf clipping: A new method to reduce papr in ofdm systems," *Information*, vol. 11, no. 4, p. 190, 2020.

[24] R. Sayyari, J. Pourrostam, and H. Ahmadi, "Efficient papr reduction scheme for ofdm-noma systems based on dsi & precoding methods," *Physical Communication*, vol. 47, p. 101372, 2021.

[25] P. Mazumder, S. Chandra, S. Rana, M. Mukhopadhyay, M. K. Naskar, *et al.*, "Par- allel hardware implementation of walsh hadamard transform," *Journal of Scientific & Industrial Research*, vol. 81, no. 07, pp. 748–753, 2022.

[26] K. Premkumar, H. Twinky, S. Naveen, M. Kathiresan, and R. Aravind, "A secured communication in watermarking using fast walsh hadamard transformation in image processing," in *2022 6th International Conference on Electronics, Communication and Aerospace Technology*, pp. 1186–1191, IEEE, 2022.

[27] S. S. Mardan and M. T. Hamood, "New fast walsh–hadamard–hartley transform algorithm," *International Journal of Electrical and Computer Engineering*, vol. 13, no. 2, p. 1533, 2023.

[28] M. Lopez-Ramirez, C. Rodriguez-Donate, L. M. Ledesma-Carrillo, F. J. Villalobos-Pina, J. U. Munoz-Minjares, and E. Cabal-Yepez, "Walsh–hadamard domain-based intelligent online fault diagnosis of broken rotor bars in induction motors," *IEEE Transactions on Instrumentation and measurement*, vol. 71, pp. 1–11, 2022.

[29] N. Patra and S. S. Nayak, "Discrete hartley transform and its applications-a review," *Journal of Integrated Science and Technology*, vol. 10, no. 2, pp. 173–179, 2022.

[30] M. WU, Y. XIE, Y. SHI, J. ZHANG, T. YAO, and W. LIU, "An adaptively biased ofdm based on hartley transform for visible light communication systems," *IEICE*

Transactions on Fundamentals of Electronics, Communications and Computer Sci- ences, 2023.

[31] Z. Wang and S. Chen, “Ber performance analysis of an ofdm-based visible light communication system using dht post-coding,” *Optoelectronics letters*, vol. 18, no. 5, pp. 288–292, 2022.

[32] R. M. Holla and D. Suma, “Progressive hartley image secret sharing for high-quality image recovery,” *Cogent Engineering*, vol. 10, no. 2, p. 2262805, 2023.

[33] K. A. Bouslam, A. Khabba, F.-Z. Bennioui, J. Amadid, R. Iqdour, and A. Zeroual, “A hybrid technique based on zadoff-chu and simplified selective mapping for papr reduction in gfdm system,” in *2023 3rd International Conference on Innovative Re- search in Applied Science, Engineering and Technology (IRASET)*, pp. 1–5, IEEE, 2023.

[34] D. Gregoratti, X. Arteaga, and J. Broquetas, “Mathematical properties of the zadoff- chu sequences,” *arXiv preprint arXiv:2311.01035*, 2023.

[35] C. Sharma and P. Sharma, “Performance enhancement of generalized frequency divi- sion multiplexing using zadoff-chu precoding scheme,” *Turkish Journal of Computer and Mathematics Education (TURCOMAT)*, vol. 13, no. 03, pp. 1059–1067, 2022.

[36] S. L. Chukkaluru and S. Affijulla, “Review of discrete fourier transform during dy- namic phasor estimation and the design of synchrophasor units,” *ECTI Transac- tions on Electrical Engineering, Electronics, and Communications*, vol. 21, no. 1, pp. 248548–248548, 2023.

[37] E. Rajaby and S. M. Sayedi, “A structured review of sparse fast fourier transform algorithms,” *Digital Signal Processing*, vol. 123, p. 103403, 2022.

[38] G. Fan, Z. Yu, Z. Shuangshuang, L. Yue, C. Xiao, Z. Chao, W. Xiang, and Z. Zhen, “An improved discrete fourier transformation channel estimation algorithm with low complexity for orthogonal frequency division multiplexing-based power line carrier communication systems,” *IET Communications*, vol. 17, no. 16, pp. 1907–1916, 2023.

[39] C. Scribano, G. Franchini, M. Prato, and M. Bertogna, “Dct-former: Efficient self-attention with discrete cosine transform,” *Journal of Scientific Computing*, vol. 94, no. 3, p. 67, 2023.

[40] O. Popov, T. Chernysheva, K. Orlov, and P. Sapronov, “Algorithm for the complex discrete cosine transform,” in *2022 Intelligent Technologies and Electronic Devices in Vehicle and Road Transport Complex (TIRVED)*, pp. 1–7, IEEE, 2022.

[41] M. Ulicny, V. A. Krylov, and R. Dahyot, “Harmonic convolutional networks based on discrete cosine transform,” *Pattern Recognition*, vol. 129, p. 108707, 2022.

[42] M. Okade and J. Mukherjee, "Discrete cosine transform: A revolutionary transform that transformed human lives [cas 101]," *IEEE Circuits and Systems Magazine*, vol. 22, no. 4, pp. 58–61, 2022.

[43] W. Burger and M. J. Burge, "The discrete cosine transform (dct)," in *Digital Image Processing: An Algorithmic Introduction*, pp. 589–597, Springer, 2022.

[44] C. Li, Y. Ren, G. Long, E. Boerman, and S. Zhao, "A fast sine transform accelerated high-order finite difference method for parabolic problems over irregular domains," *Journal of Scientific Computing*, vol. 95, no. 2, p. 49, 2023.

[45] H. Zeng, Z. Cai, P. Zheng, H. Liu, and W. Luo, "Secure evaluation of discrete sine transform in homomorphic encrypted domain," in *International Conference on Artificial Intelligence and Security*, pp. 513–525, Springer, 2022.

[46] T. Suzuki, S. Kyochi, and Y. Tanaka, "Regularity-constrained fast sine transforms," *IEEE Signal Processing Letters*, vol. 29, pp. 1744–1748, 2022.

[47] D. Wu, X. Wang, and S. Wu, "A hybrid framework based on extreme learning machine, discrete wavelet transform, and autoencoder with feature penalty for stock prediction," *Expert Systems with Applications*, vol. 207, p. 118006, 2022.

[48] S. H. Syed and V. Muralidharan, "Feature extraction using discrete wavelet transform for fault classification of planetary gearbox–a comparative study," *Applied Acoustics*, vol. 188, p. 108572, 2022.

[49] S. Momeneh and V. Nourani, "Application of a novel technique of the multi-discrete wavelet transforms in hybrid with artificial neural network to forecast the daily and monthly streamflow," *Modeling Earth Systems and Environment*, vol. 8, no. 4, pp. 4629–4648, 2022.